



# Biochemical characterization of an esterase from *Clostridium acetobutylicum* with novel GYSMG pentapeptide motif at the catalytic domain

Vijayalakshmi Nagaroor<sup>1</sup> · Sathyanarayana N. Gummadi<sup>1,2</sup>

Received: 14 July 2019 / Accepted: 25 November 2019 / Published online: 5 December 2019  
© Society for Industrial Microbiology and Biotechnology 2019

## Abstract

Gene CA\_C0816 codes for a serine hydrolase protein from *Clostridium acetobutylicum* (ATCC 824) a member of hormone-sensitive lipase of lipolytic family IV. This gene was overexpressed in *E. coli* strain BL21 and purified using Ni<sup>2+</sup>-NTA affinity chromatography. Size exclusion chromatography revealed that the protein is a dimer in solution. Optimum pH and temperature for recombinant *Clostridium acetobutylicum* esterase (Ca-Est) were found to be 7.0 and 60 °C, respectively. This enzyme exhibited high preference for *p*-nitrophenyl butyrate.  $K_M$  and  $k_{cat}/K_M$  of the enzyme were 24.90 μM and 25.13 s<sup>-1</sup> μM<sup>-1</sup>, respectively. Sequence analysis of Ca-Est predicts the presence of catalytic amino acids Ser 89, His 224, and Glu 196, presence of novel GYSMG conserved sequence (instead of GDSAG and GTSAG motif), and undescribed variation of HGSG motif. Site-directed mutagenesis confirmed that Ser 89 and His 224 play a major role in catalysis. This study reports that Ca-Est is hormone-sensitive lipase with novel GYSMG pentapeptide motif at a catalytic domain.

**Keywords** *Clostridium acetobutylicum* · Esterase · Purification · Biochemical characterization · Kinetics

## Introduction

Lipolytic enzymes (E.C. 3.1.1.x) include lipases and esterases that can hydrolyze the ester linkage and are also involved in the transesterification process [1–3]. Both enzymes share common  $\alpha/\beta$  hydrolase structural fold and serine protease catalytic mechanism, but differ in substrate specificity. They are widely distributed in all life forms [4–6]. These lipolytic enzymes have a broad range of industrial applications because of unique features such as high regio, enantio, stereoselectivity, broad substrate specificity,

stability in organic solvents, aiding synthesis of biodegradable compounds, and non-requirement of cofactors which also makes them attractive biocatalyst [7–11]. In bacteria, eight classes of lipolytic enzymes have been classified based on protein sequences and biochemical properties [4, 12]. Of these, the  $\alpha/\beta$  hydrolase fold superfamily of proteins was categorized into four blocks namely C, H, L, and X which stands for carboxylesterases, hormone-sensitive lipases (HSL), lipases, and X stands for other proteins that has alpha-beta hydrolase fold [13, 14] by the ESTHER database.

In mammals, HSL plays major role in lipid metabolism, cholesterol metabolism, and steroidogenesis by stimulation of hormones such as catecholamines, glucagon, and adrenocorticotropic hormones [15, 16]. Structurally, mammalian HSL consists of an amino-terminal domain that contributes to protein-protein interactions and carboxyl-terminal domain which is involved in catalytic function [17, 18]. This highly conserved catalytic domain is analogous to some of the microbial proteins which are referred to as microbial hormone-sensitive lipase (HSL) [18, 19]. The catalytic domain consists of an alpha-beta hydrolase fold, with catalytic residues Ser-Asp/Glu and His that plays a major role in catalysis. Catalytic serine residue is conserved in the G-X-S-X-G pentapeptide motif [20, 21]. Another short highly conserved

**Electronic supplementary material** The online version of this article (<https://doi.org/10.1007/s10295-019-02253-8>) contains supplementary material, which is available to authorized users.

✉ Sathyanarayana N. Gummadi  
gummadi@iitm.ac.in

<sup>1</sup> Applied and Industrial Microbiology Laboratory (AIM Lab), Department of Biotechnology, Bhupat and Jyoti Mehta School of Biosciences, Indian Institute of Technology Madras, Chennai 600 036, India

<sup>2</sup> Present Address: AIM Lab, Department of Biotechnology, IIT Madras, Chennai 600 036, India

HGGG motif is present upstream to the highly conserved pentapeptide motif that stabilizes the oxyanion intermediate during the hydrolysis [22, 23].

Most of the microbial HSL are esterases rather than lipases [24]. Microbial HSL are categorized into two sub-families viz. GTSAG and GDSAG based on the serine conserved around pentapeptide motifs [24, 25]. In several studies, microbial HSL have been reported from various microbes such as *Salinisphaera* sp. [26], *Bacillus* [23], *Rhizomucor* [27], *Archaeoglobusfulgidus* [28], *Mycobacterium tuberculosis* [29], metagenomic source [30], *Rheinheimerasp* [31], *Bjerkanderaadusta* [32], and *Lactobacillus plantarum* WCFS1 [33].

In our investigation, we found that the genome of *Clostridium acetobutylicum* (ATCC 824) encodes numerous ORFs encoding putative esterases/lipases. Amongst them, the gene CA\_C0816 which is 729 nucleotides encodes lipase/esterase-related protein containing 242 amino acids. The crystal structure of this protein is available with PDB ID 3E0X. However, the biochemical properties and functions of this enzyme have not been studied. Based on the sequence alignment, it was found that the Ca-Est belonged to lipolytic family IV of hormone-sensitive lipase. An effort has been made to study the overexpression, purification, biochemical characterization, and identification of catalytic serine residue in this study.

## Materials and methods

### Chemicals

Isopropyl thio- $\beta$ -D-galactoside (IPTG), *p*-Nitrophenyl esters, phenyl acetate,  $\alpha$ -naphthyl acetate,  $\beta$ -naphthyl acetate, and 4-methyl umbelliferyl acetate were procured from SIGMA ALDRICH (USA). Ni-NTA resin for affinity chromatography was purchased from Qiagen, Germany. Standard proteins for size exclusion chromatography were purchased from Bio-Rad laboratories (USA). PCR primers were procured from Bio Serve, India. Other reagents and chemicals were procured from Himedia.

### Sequence alignment

Amino acid sequence similarity and alignment were carried with closely related homologs using the Clustal omega program.

### Plasmid, bacterial strains, and maintenance

*Escherichia coli* DH5 $\alpha$  possessing pMCSG7 contains the gene coding for lipase/esterase from *Clostridium acetobutylicum* (ATCC 824). The clone (ID: caCD00398108) was

procured from the DNASU plasmid repository. *E. coli* BL21 (DE3) was used for the recombinant expression of the lipase/esterase gene. Recombinant *E. coli* strains were maintained on ampicillin (100  $\mu$ g/ml) containing LB agar media.

### Overexpression and purification of recombinant Ca-Est

Plasmid pMCSG7 harboring lipase/esterase gene from *Clostridium acetobutylicum* was isolated from *E. coli* DH5 $\alpha$  using plasmid isolation kit (Qiagen). Isolated plasmid DNA was transformed into *E. coli* strain BL21 (DE3) and the transformed cells were selected based on their survival on LB media containing ampicillin (100  $\mu$ g/ml). Recombinant strains were cultured overnight in LB media with ampicillin (100  $\mu$ g/ml) at 37 °C, 180 rpm on a rotary shaker. For overexpression of Ca-Est, cells were induced with 0.3 mM IPTG once A<sub>600</sub> of cells reached ~0.8. After induction, the effect of post-incubation temperature (15 °C, 22 °C and 37 °C) and post-incubation period (4, 6, 10, and 18 h) on protein expression were studied. Induced cells were harvested from media by centrifugation and were preserved at –80 °C for further studies.

For extraction of recombinant protein, cells were resuspended in cell lysis buffer containing 0.05 M sodium phosphate buffer pH 7.0, NaCl 0.3 M, 1 mM PMSF, 1 mM EDTA, and 1 mM DTT. Cell lysis was carried out by sonication (Vibrocell Ultrasonicator) on ice for 5 min at 37% amplitude with pulse 2 s on and 4 s off. The cell lysate was centrifuged at 4 °C for 45 min at 12,000 rpm to remove cell debris and inclusion bodies. The supernatant containing recombinant protein was loaded onto 2 ml of Ni<sup>2+</sup>-NTA resin that was previously equilibrated with lysis buffer (0.05 M sodium phosphate buffer pH 7.0, 0.3 M NaCl). The column was placed on a rocker 4 °C for 3 h for efficient binding of the protein to the resin. Flow-through was collected, followed by a wash with 20 mM imidazole to remove the weakly bound unwanted proteins. The recombinant protein, that was bound to the resin, was eluted with 100 mM imidazole [34]. To remove imidazole, the eluted recombinant protein was kept for dialysis. Concentration of protein was estimated by BCA method using BSA as standard and was preserved at –80 °C. This protocol was also used for the overexpression and purification of Ser89Ala and His224Ala mutants.

### Determination of molecular mass and oligomeric state of the protein by size exclusion chromatography

Superdex 200 (GE Healthcare) column, previously equilibrated with 0.05 M sodium phosphate buffer at pH 7.0, was injected with purified protein and eluted fractions were

collected at a flow rate of 0.75 ml/min. The molecular mass of protein was determined from the calibration curve using the standard proteins (Bio-Rad Catalog # 1511901).

### Lipase/esterase assay

Lipase/esterase activity of recombinant protein was estimated by measuring the continuous release of *p*-nitrophenol from *p*-nitrophenyl esters (*p*-NP esters) at 348 nm (isobestic point) in a UV spectrophotometer (Perkin Elmer Lambda 25 UV/VIS spectrophotometer, USA). The reaction was done in 1 ml of reaction mixture containing 1 mM of (*p*-NPA) (stock was dissolved in acetonitrile) in 0.05 M of sodium phosphate buffer at pH 7.0 and the required amount of purified recombinant protein at 37 °C. 1 unit of enzymatic activity was defined as the amount of purified protein used to release 1 μmol of *p*-nitrophenol/min. The molar absorptivity of *p*-nitrophenol at 348 nm was experimentally determined to be 5.3 mM<sup>-1</sup> cm<sup>-1</sup> and the same was used for calculating enzyme activity. All the assays were carried out in triplicates for statistical significance.

### Effect of the amount of enzyme, pH, and temperature on Ca-Est activity

To determine the amount of an enzyme for optimum activity, assays were carried out with varying amounts of an enzyme such as 12, 25, 50, 100, and 500 ng at a constant temperature of 37 °C and pH 7.0 with 1 mM *p*-NPA as substrate. To identify optimum pH of the enzyme, experiments were carried out at constant temperature 37 °C using buffers of various pHs ranging from 4.5 to 9.0 [(citrate buffer pH 4.5–6.0), (sodium phosphate buffer pH 6.5–8.0), (Tris—HCl pH 8.5–9.0)] with 25 ng of protein. To determine the temperature optimum for an enzyme, experiments were performed using 25 ng of protein at a constant pH 7.0 with temperatures ranging from 20 °C to 80 °C.

### Thermal stability

Thermal stability of wild type Ca-Est was checked by incubating the pure enzyme diluted with 0.5 M sodium phosphate buffer a pH 7.0 at various temperatures 30 °C, 60 °C, and 80 °C up to 6 h. At different time intervals, enzyme sample was taken and incubated at 4 °C and the residual enzyme activity was measured using *p*-nitrophenyl butyrate as substrate under optimized assay conditions.

### Substrate specificity of wild Ca-Est and mutants

To determine whether the recombinant Ca-Est belonged to esterase or lipase, substrate specificity was studied with substrates of varying acyl lengths such as *para*-nitrophenyl

acetate (*p*-NPC2), *para*-nitrophenyl butyrate (*p*-NPC4), *para*-nitrophenyloctonate (*p*-NPC8), *para*-nitrophenyldecanoate (*p*-NPC10), *para*-nitrophenyldodecanoate (*p*-NPC12), and *para*-nitrophenyl palmitate (*p*-NPC16). These substrates were dissolved in acetonitrile to obtain stock solution of 10 mM. Aryl esterase activity was determined using aromatic esters such as phenyl acetate, α-naphthyl acetate, β-naphthyl acetate, and 4-methyl umbelliferyl acetate. Hydrolysis of α-naphthyl acetate, β-naphthyl acetate, 4-methyl umbelliferyl acetate, and phenylacetate was carried out by measuring the absorbance of α-naphthol at 235 nm, β-naphthol at 330 nm 4-methyl umbelliferone at 340 nm, and phenol at 270 nm. Thioesterase activity was determined using phenyl thioacetate as a substrate. Hydrolysis of phenyl thioacetate was monitored by measuring the absorbance of 2-nitro-5 thiobenzoate at 410 nm. 1 mM phenyl thioacetate was dissolved in ethanol containing 0.25 mM 2,2'-Dinitro-5,5'-dithiobenzoic acid (DTNB).

The reaction was performed in 1 ml of reaction mixture contains 0.5 mM of *p*-nitrophenyl esters in 0.05 M sodium phosphate buffer at pH 7.0 and 25 ng of purified protein at 60 °C at 348 nm. The substrate specificity of mutants Ser89Ala and His224Ala was estimated by similar protocol.

### Kinetic parameters

Kinetic parameters of enzyme viz.,  $K_M$ ,  $V_{max}$ , and  $k_{cat}/K_M$  were investigated using *p*-NP acetate, *p*-NP butyrate and α-naphthyl acetate as substrates within the range of 5–400 μM under optimized assay conditions (temperature 60 °C and pH 7.0 with 25 ng of protein). The kinetic parameters  $K_m$ ,  $V_{max}$ , and  $k_{cat}/K_m$  were analyzed using non-linear regression analysis with Graph Pad Prism 5.

### Effect of amino acid modifiers, detergents, solvents, and metal ions on Ca-Est

The effect of various amino acid modifying reagents on the activity of Ca-Est was tested in the presence of 10 mM of phenylmethylsulfonyl fluoride (PMSF) for serine, diethylpyrocarbonate (DEPC) for histidine, phenyl glyoxal hydrate (PGH) for arginine, 1-(3-dimethylaminopropyl)3-ethyl carbodiimide hydrochloride (EDAC) for aspartic acid, and dithiothreitol (DTT) for thiol group. The activity was performed using *p*-NPB as substrate under optimized assay conditions.

To study the effect of various detergents on Ca-Est activity, enzyme assays were carried out with 1% (v/v) sodium dodecyl sulfate (SDS), sodium deoxycholate (SDC), Brij 35, Triton X, Tween 80, and at Tween 20 in the assay mixture. The activity was performed using *p*-NPB as a substrate under optimized assay conditions.

To determine the effect of organic solvents on Ca-Est activity enzyme assays were carried out with 10% (v/v)

ethanol, methanol isopropanol acetone, and DMSO under optimized assay conditions. The effect of various metals ions on Ca-Est activity was determined with 1 mM metal ions such as  $Mn^{2+}$ ,  $Cu^{2+}$ ,  $Fe^{2+}$ ,  $Ni^{2+}$ ,  $Zn^{2+}$ ,  $Mg^{2+}$ ,  $Na^+$ , and  $K^+$  under optimized assay conditions. The activity was performed using *p*-NPB under optimized assay conditions. In all cases, the activity of an enzyme in the absence of modifiers, detergents, metal ions, and organic solvents was considered as control.

### Identification of catalytic residues in Ca-Est by site-directed mutagenesis

To identify the catalytic residues in the Ca-Est, site-directed mutagenesis was carried out on the pMCSG7 vector carrying the esterase gene using a PCR-based method. Amino acid serine positioned at 89 and histidine 224 were mutated to alanine. The following primers were designed to introduce mutations: forward primers Ser89Ala: (5'ATTGGA TATGCCATGGGGGAGC-3') and Ser89Ala reverse primers: (5'CCCCCATGGCATATCCAATTAA-3') and His224Ala forward primers: (5'CCGGTAAGGCTTTCCTATTA GTAGTAA-3') and reverse primers: (5'ATAGGAAAGC CTTACCGGTTTCAAAGA-3'). (position of the mutated codons are underlined). The mutant plasmid was generated by PCR with the following conditions: 98 °C for 60 s was kept for initial denaturation, amplification process for 30 cycles (95 °C for 30 s, 56 °C for 45 s, 72 °C for 6 min), and 72 °C for 20 min, for final elongation. After amplification, the product was digested with enzyme Dpn-I followed by transformation into *E. coli* DH5 $\alpha$ . Positives clones were screened by Sanger's method of DNA sequencing. Similarly, the mutants Ser89Ala and His224Ala were overexpressed and purified as that of wild type.

### CD spectra studies

To determine secondary structure of the protein, CD spectra were measured using JASCO J-810 spectro polarimeter (Easton, MD) with Peltier temperature control maintained at 20 °C and 60 °C. Far UV CD spectra was measured in the wavelength range of 200–250 nm with a scanning speed of 10 nm/min. Sodium phosphate buffer at pH 7.0 was used as a blank for spectral correction. The concentration of protein used was 0.2 mg/ml for recording the spectra. The thermal denaturation of protein was analyzed by monitoring the changes in molar ellipticity at 222 nm using Jasco J-815 spectropolarimeter. The protein was diluted 0.02 mg/ml in 0.05 M sodium phosphate buffer at pH 7.0 and subjected to increase in temperature from 20 to 100 °C at a scan rate of 10 nm/min. To calculate  $T_m$  fraction unfold was plotted against temperature and fitting the curve against Boltzmann sigmoidal equation using GraphPad Prism 6.

### Statistical analysis

All the experiments were performed as at least three independent experiments. Statistical significance was determined by Dunnett's multiple comparison test using Graph pad prism.  $p < 0.05$  was considered statistically significant.

### Docking analysis

Molecular docking simulations were performed using Auto-dock 4.2. The crystal structure of Ca-Est from *Clostridium acetobutylicum* (ATCC824) with a resolution of 1.45 Å° (PDB ID:3E0X) was downloaded from Protein Data Bank and ligand (*p*-Nitrophenyl butyrate) from zinc data bank. *p*-Nitrophenyl butyrate was docked against canonical binding site of the protein.

## Results

### Overexpression and purification of Ca-Est

The recombinant plasmid pMCSG7 harboring lipase/esterase gene *Clostridium acetobutylicum* was overexpressed in *E. coli* BL21. It was found at 22 °C and 18 h maximum soluble fraction of recombinant Ca-Est was obtained (data not shown) and these conditions were, therefore, designated as optimal for overexpression. The recombinant protein was purified using Ni–NTA affinity chromatography. 100 mM imidazole was used for elution of bound Ca-Est with theoretical molecular mass 27.14 kDa. The recombinant esterase appeared as a single band of 29 kDa on Coomassie brilliant blue-stained SDS PAGE (Fig. 1a). The native molecular mass and oligomeric state of protein were depicted as a single elution peak with 49.67 kDa of molecular mass by size exclusion chromatography, suggesting that the protein exists as a homodimer (Fig. 1b, c).

### Effect of amount of protein, temperature, and pH on Ca-Est activity

The recombinant enzyme showed maximum specific activity when 25 ng ( $425 \pm 13.86$  U/mg) of purified protein was used in the assay (Fig. 2a). Hence, enzyme amount of 25 ng was used as optimum amount in subsequent studies. Ca-Est activity was studied at various pH, and maximum specific activity ( $525 \pm 23.02$  U/mg) was obtained at pH 7.0. At pH 4.5 and 9.0, maximum specific activities retained were 26% and 60% of maximum activity, respectively, at pH 7.0 (Fig. 2b). Similarly, the effect of temperature was also studied and it was found that there was an increase in activity with temperature increase from 20 to 60 °C and maximum activity ( $821 \pm 34.49$  U/mg) was

**Fig. 1** Purification of Ca-Est from *Clostridium acetobutylicum*. **a** 12% SDS PAGE analysis of recombinant lipase/esterase gene from *Clostridium acetobutylicum* was overexpressed in *E. Coli* BL21 (DE3) cells purified by affinity chromatography with Ni–NTA matrix: Lane M: protein marker (Molecular weight in kDa) lane 1: induced whole cell lysate, lane 2: pellet, lane 3 supernatant, lane 5: Flow-through, lane 4: 10 mM Imidazole wash, lane 6: 20 mM Imidazole wash and lane 7: 100 mM elution. Each lane contains 10  $\mu$ L of the fraction. **b** Analysis of the oligomeric state of Lipase/esterase by gel filtration chromatography: Gel filtration chromatogram was obtained by plotting with A280 versus with its corresponding elution volume. **c** Semilog plot of molecular masses of the standards used versus with elution volume. The molecular mass and oligomeric state of the esterase were found using the slope and intercept of a standard plot

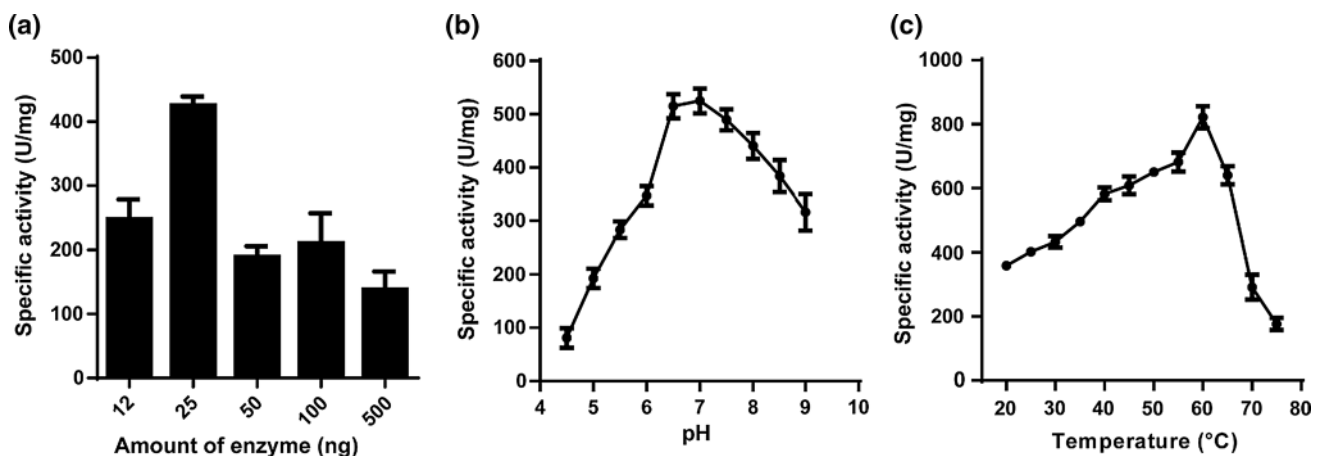
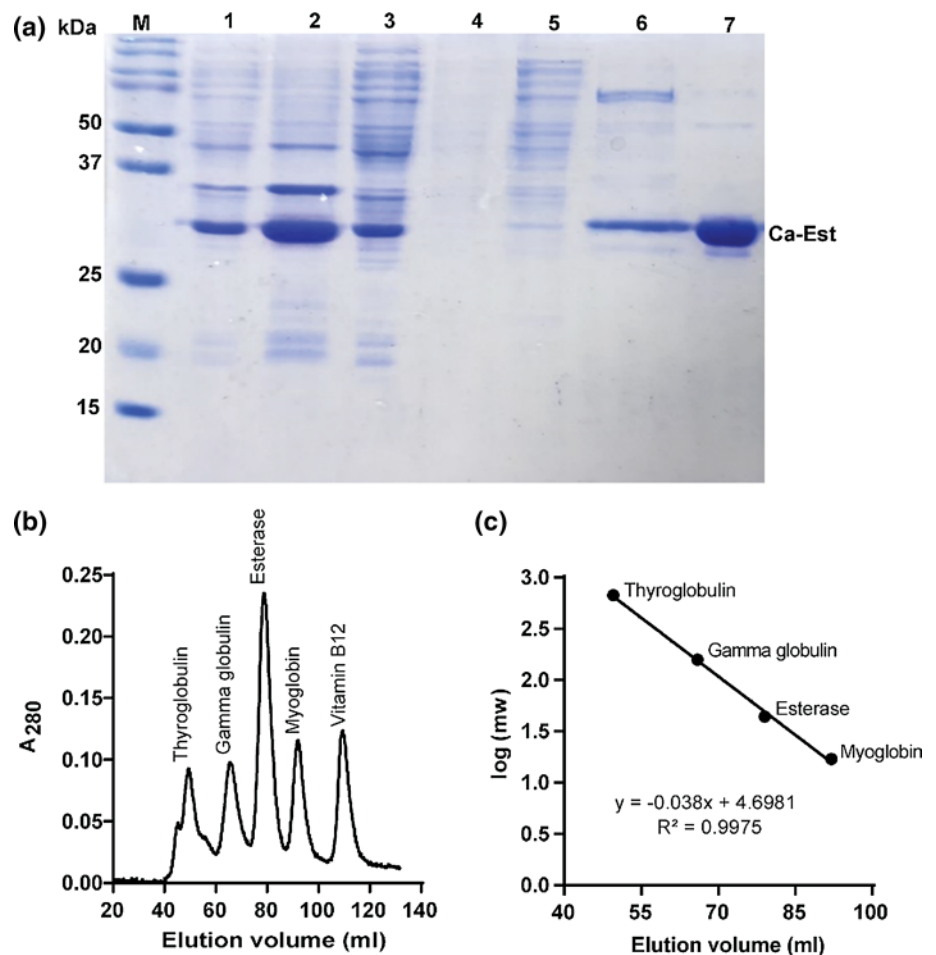


**Fig. 2** Biochemical characterization of the recombinant Ca-Est. Effect of the **a** amount of enzyme **b** pH **c** temperature on the recombinant Ca-Est activity. The assay was performed using 1 mM *p*-nitro-

phenyl acetate as a substrate in 50 mM sodium phosphate buffer at pH 7.0. Results are the mean  $\pm$  SD from triplicate experiments

obtained at 60  $^{\circ}$ C (Fig. 2c). At 20  $^{\circ}$ C and 65  $^{\circ}$ C, the specific activity was 56% and 78% of its maximum activity at an optimum temperature of 60  $^{\circ}$ C. The specific activity dropped drastically beyond 65  $^{\circ}$ C. Thermal stability of

wild-type Ca-Est suggested that the enzyme was stable at 30  $^{\circ}$ C with  $t_{1/2}$  of 533 min. The  $t_{1/2}$  of enzyme at 60  $^{\circ}$ C and at 80  $^{\circ}$ C was found to be 17.86 min and 1.39 min respectively (Fig. 5b).

## Substrate specificity of Ca-Est and kinetic parameters

Using various acyl lengths of *p*-nitrophenyl esters, aromatic esters and phenyl thioacetate the substrate specificity for wild-type Ca-Est was studied. It was observed that the maximum specific activity was towards *p*-nitrophenyl butyrate (C4). There was no detectable enzymatic activity towards *p*-nitrophenyldecanoate (pNPC10), *p*-nitrophenyl-dodecanoate (pNPC12) *p*-nitrophenyl palmitate (pNPC16) and phenyl acetate. This showed that the recombinant enzyme has an affinity towards short-chain acyl length of *p*-nitrophenyl esters confirming that CA-C0816 encoding gene is an esterase (Fig. 3a) (Table 1). Kinetic studies on the Ca-Est followed simple hyperbolic MichaelisMenten kinetics for the substrates *p*-NPA *p*-NPB, and  $\alpha$  naphthyl acetate (Fig. 3b). Kinetic constants  $K_M$ ,  $V_{max}$ , turnover number ( $k_{cat}$ ), and catalytic efficiency ( $k_{cat}/K_M$ ) were calculated for various substrates by fitting the kinetic data on a non-linear regression by using Graph Pad Prism 5.0 (Table 2). It was found that the recombinant enzyme showed more affinity towards *p*-NPB (C4) than *p*-NPA (C2) and  $\alpha$  naphthyl acetate.

## Effect of amino acid modifiers on Ca-Est activity

The effect of various amino acid modifying agents such as PMSF for Serine, DEPC for histidine EDAC for aspartic acid, PGH for arginine and DTT for thiol group, on the recombinant Ca-Est was studied. The treatment of serine modifier results in loss of 78% esterase activity, whereas histidine modifier showed complete inhibition of esterase activity (Fig. 4a). The thiol modifier showed a 62% loss of activity and the arginine modifier showed a 40% loss of

**Table 1** Biochemical assay for the Ca-Est using various substrates

Substrates	Specific activity (U/mg)
<i>p</i> -Nitrophenyl acetate	1386 ± 10.7
<i>p</i> -Nitrophenyl butyrate	2280 ± 20.8
<i>p</i> -Nitrophenyl octonate	326 ± 38.85
<i>p</i> -Nitrophenyl decanoate	ND
<i>p</i> -Nitrophenyl dodecanoate	ND
<i>p</i> -Nitrophenyl palmitate	ND
$\alpha$ -Naphthyl acetate	770 ± 7.35
$\beta$ -Naphthyl acetate	145 ± 15.11
4-Methylumbelliferyl acetate	202 ± 22.45
Phenyl acetate	ND
Phenyl thioacetate	13 ± 0.00

Enzyme activities were determined at 60 °C in 50 mM sodium phosphate buffer (pH 7.0) using various substrates. Results are the mean ± SD of three independent experiments

ND not determined

activity (Fig. 4a). Amongst all, aspartate modifier had least effect on enzyme activity (Fig. 4a).

## Effect of various additives on Ca-Est activity

Ca-Est activity was studied in the presence of various detergents to be effective for stain removal on fabric and dish wash cleaning. On comparison with control, SDS showed that 23% of loss of inhibition was observed with SDS and loss in activity with Tween 80 and Triton X were 26% and 28%, respectively (Fig. 4b). SDC and Tween 20 showed 13% and 19% inhibition, whereas Brij 35 had shown no effect

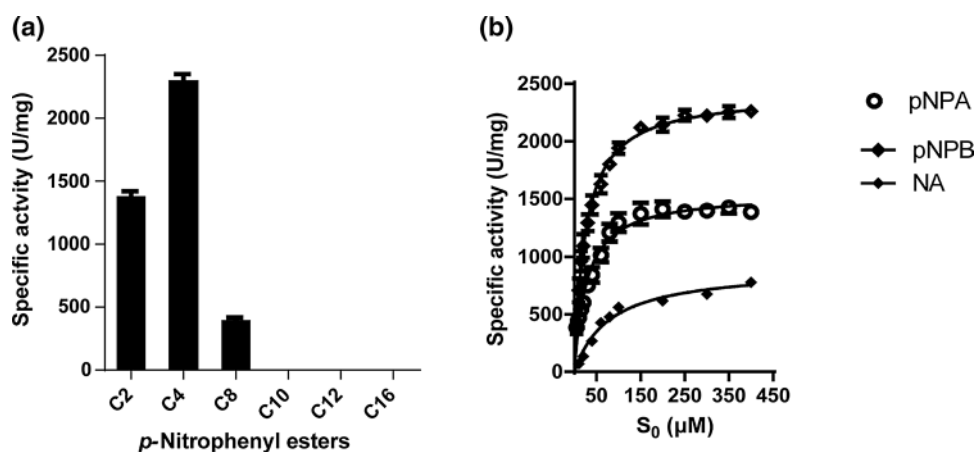


**Fig. 3** Determination of substrate specificity and kinetic parameters. **a** Substrate specificity of Ca-Est towards various *p*-nitrophenyl esters (0.5 mM) were assayed at 60 °C in the 50 mM sodium phosphate buffer at pH 7.0. No activity was detected for the acyl length of 16 carbon. Results are the mean ± SD of three experiments done in trip-

licates. **b** Michaelis–Menten plots of a recombinant esterase from *Clostridium acetobutylicum*. Kinetic data are measured using a UV spectrophotometer using *p*-NPC2 (circle) and *p*-NPC4 (square). The assay was conducted at 50 mM phosphate buffer at pH 7.0 and 60 °C

**Table 2** Kinetic parameters for *p*-NPA and *p*-NPB hydrolysis by Ca-Est

Substrate	$V_{\max}$ ( $\mu\text{mol min}^{-1} \text{mg}^{-1}$ )	$K_m$ ( $\mu\text{M}$ )	$k_{\text{cat}}$ ( $\text{s}^{-1}$ )	$k_{\text{cat}}/K_m$ ( $\text{s}^{-1} \mu\text{M}^{-1}$ )
<i>p</i> -NPA	$1561 \pm 23.02$	$27.3 \pm 0.64$	$754 \pm 11.12$	$27.67 \pm 0.88$
<i>p</i> -NPB	$24,066 \pm 31.01$	$25.13 \pm 2.31$	$1162 \pm 14.9$	$46.91 \pm 3.63$
$\alpha$ -naphthyl acetate	$779 \pm 7.31$	$73.82 \pm 2.85$	$375 \pm 3.58$	$207 \pm 0.2$

Enzyme activities were determined at 60 °C in 50 mM sodium phosphate buffer (pH 7.0) using *p*-nitrophenyl acetate and *p*-nitrophenyl butyrate. Results are the mean  $\pm$  SD of three independent experiments

**Fig. 4** Effect of additives on recombinant Ca-Est. **a** aminoacid modifiers, **b** detergents, **c** solvents, and **d** metal ions on Ca-Est activity. Enzymatic activity was performed at 60 °C in 50 mM sodium phosphate buffer at pH 7.0 with *p*-NPC4. Results are the mean  $\pm$  SD from three independent experiments. Asterisks (\*) indicates  $p < 0.05$

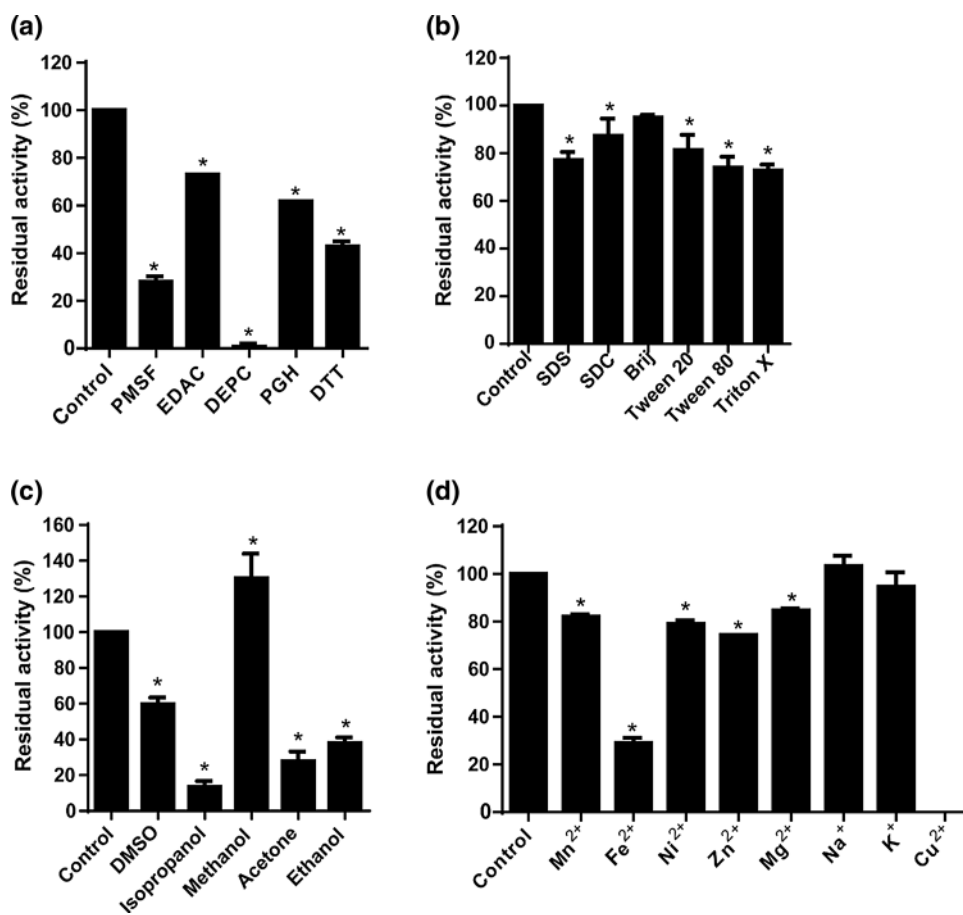


(Fig. 4b). Significant inhibition was observed with 10% isopropanol, acetone, and ethanol. DMSO showed 50% inhibition of Ca-Est activity. However, methanol was found to enhance the esterase activity by 10% when compared with control (Fig. 4c). Metal ions such as  $\text{Na}^+$  and  $\text{K}^+$  showed negligible effect.  $\text{Mn}^{2+}$ ,  $\text{Ni}^{2+}$ ,  $\text{Zn}^{2+}$ , and  $\text{Mg}^{2+}$  inhibited the enzyme activity ( $\sim 20\%$ ). Interestingly,  $\text{Fe}^{2+}$  showed  $\sim 75\%$  loss of activity and complete inhibition of esterase activity was observed with  $\text{Cu}^{2+}$  (Fig. 4d).

### Secondary structure of Ca-Est

The secondary structure of the Ca-Est was studied by circular dichroism spectra. The far UV spectra displayed a double peak at 208 and 222 nm, indicating that the protein

has stable conformation of secondary structure at 25 and 60 °C (Fig. 5c). The melting temperature of the protein was determined by plotting graph against fraction unfold and temperature fitted to Boltzmann curve and  $T_m$  was found to be 67.71 °C at 222 nm.

### Catalytic activity of Ser89Ala and His224Ala mutant by using *p*-NP esters

Based on the effect of amino acid modifiers, Ser89Ala and His224Ala mutants were generated and tested for enzyme activity towards various substrates similar to studies on wild type [35]. Interestingly, mutations of Ser89Ala and His224Ala showed complete inactivation of the enzyme

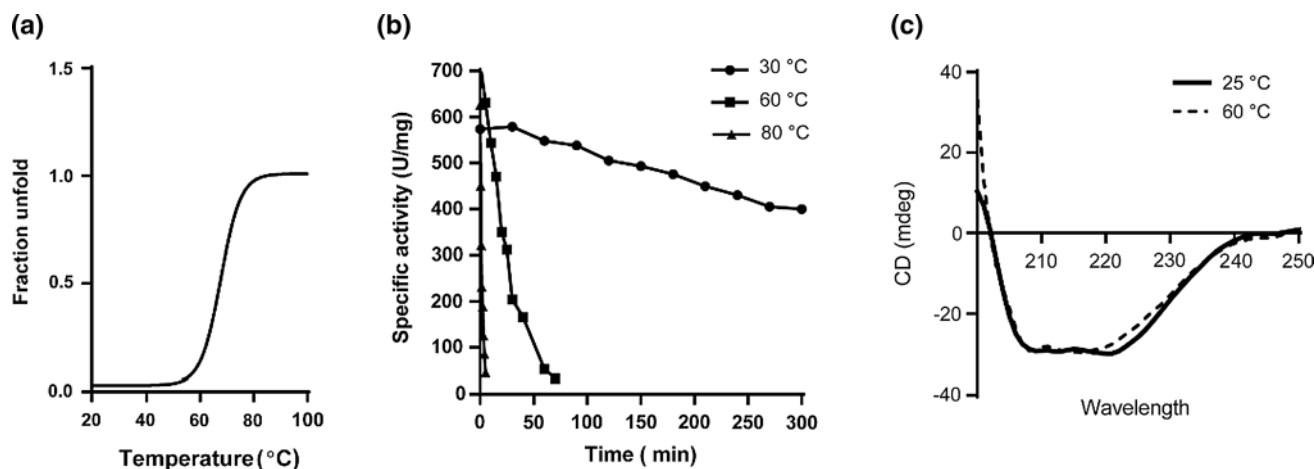


**Fig. 5** CD spectra recombinant Ca-Est. The CD spectra of recombinant Ca-Est were recorded at pH 7.0 and 25 °C and 60 °C

**Table 3** Comparison of Ca-Est activity with wild type and mutants

Enzyme	Specific activity (U/mg)		
	<i>p</i> -NPC2	<i>p</i> -NPC4	<i>p</i> -NPC8
Wild type	1386 ± 10	2208 ± 20	326 ± 38
Ser89Ala	–	–	–
His224Ala	–	–	–

Substrate specificity of the wild type was compared with its mutants, and the enzyme activity was carried out using 0.5 mM *p*-NPC2, *p*-NPC4, and *p*-NPC8 at 60 °C and 50 mM sodium phosphate buffer at pH 7.0

(Table 3). This confirms that these amino acids are important for enzymatic catalysis (Table 3).

## Discussion

Hydrolases are the important class of enzymes in industrial biotechnology. Among hydrolases, lipolytic enzymes are more important over proteases and amylases. Lipolytic enzymes include esterases and lipases are more valuable because of broader applications in various fields such as food industry, pharmaceutical, biofuels, paper and pulp, environmental bioremediation, and laundry industry, whose global market value was expected to reach \$590.5 million by 2020 [7]. Therefore, there is a need for the search of enzymes that can withstand harsh conditions such as temperature, pH, salt, and solvent tolerance for industrial applications. In search of novel enzymes, we selected industrially important organism, namely, *Clostridium acetobutylicum* (ATCC 824). It is an industrially important solventogenic microorganism for the production of acetone, butanol, and ethanol [36]. This organism encodes numerous putative lipase/esterases. It reacts to

butanol stress without affecting the central metabolism by upregulating the heat shock genes and downregulating genes for glycerophosphodiester, phosphodiesterase and in particular hypothetical gene CA\_C0816 [37]. Hence, we made an effort to characterize CA\_C0816 gene that encodes lipase/esterase from *Clostridium acetobutylicum* to explore its industrial applications.

Multiple sequence alignment of Ca-Est with the sequence of other family members showed that this protein consists of catalytic triad serine 89, histidine 224, and glutamic acid 196 and the catalytic serine conserved around GYSMG pentapeptide motif (Fig. 6). Another hallmark of HSL was short conserved HGGG motif upstream to the catalytic serine residue and plays a major role in stabilization of the oxyanion hole intermediate during catalysis [38, 39]. This recombinant Ca-Est exhibited HGSG instead of HGGG motif, which was generally found in HSL. Hence, Ca-Est forms a novel protein that belongs to lipolytic enzyme IV of hormone-sensitive lipase. It shows the significant amino acid sequence similarity to the human HSL [4].

Human HSL plays an important role in hydrolysis of stored triacylglycerol in adipose tissue under the influence of hormones such as catecholamine, adrenocorticotropic hormone, and glucagon and also hydrolysis of cholesterol esters in steroidogenic tissue. The activity is regulated by reversible protein phosphorylation [19]. Human HSL consists of amino-terminal domain, plays a role in protein–protein interactions and carboxyl-terminal domain consists of catalytic domain of  $\alpha/\beta$  hydrolase fold with catalytic residues (ser, Asp, and His) conserved. Phosphorylation sites are present in between the amino and carboxyl domain called a regulatory module. Human HSL shows no sequence homology to other mammalian lipases [18, 19]. Carboxyl-terminal domain is homologous to several other microbial proteins, hence called microbial HSL which indicated that

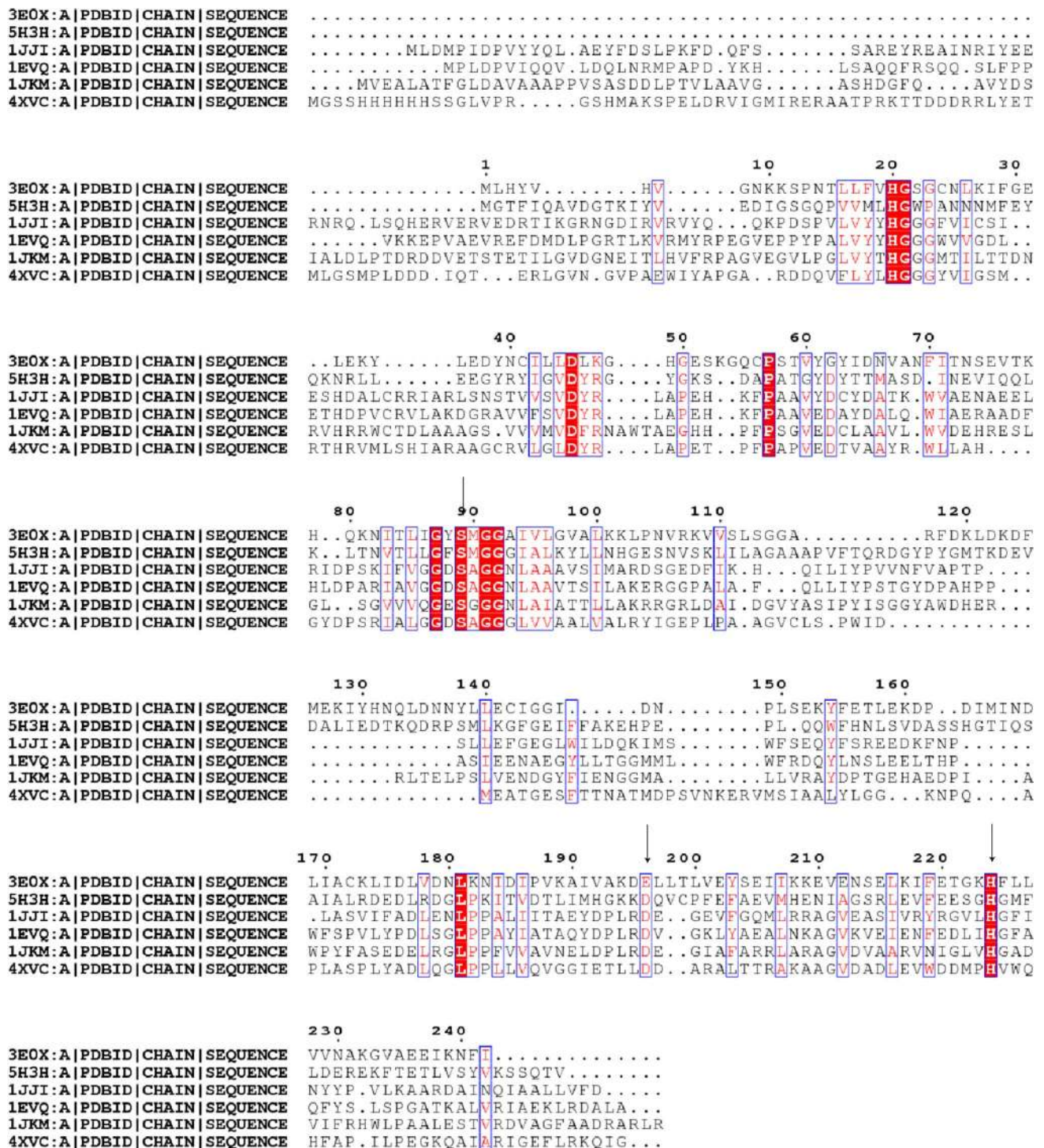


**Fig. 6** Multiple sequence alignment of amino acid esterases with other closely related esterases. The PDB codes are as follows 3E0X (from *Clostridium acetobutylicum*) 4XVC (Marine sediment genomic library), 1JKM (from *Bacillus subtilis*), 1JJI (from *Archaeoglobus-*

*fulgidus*), 1EVQ (from *Alicyclobacillus acidocaldarius*), and 5H3H (*Exiguobacterium antarcticum*). The catalytic amino acids are marked by an arrow mark

mammalian HSL are probably evolved from prokaryotic lipolytic family IV. However, the amino-terminal domain lacks similarity with other known proteins [18] (Fig.S1).

Microbial HSL has two domains namely N-terminal CAP domain that contributes in major functions such as enzyme activity, substrate specificity, thermophilicity,

regioselectivity, and thermostability [40] and C-terminal catalytic domain possesses the  $\alpha/\beta$  hydrolase fold with conserved catalytic triad in loops plays important role in catalytic mechanism and HGGG motif upstream to the catalytic serine residue, stabilizes the oxyanion intermediate. Recently, it was reported that this motif has the ability to hydrolyse tertiary alcohol esters, because it provides more space for the binding of tertiary alcohol esters [41]. The CAP domain is usually present above the  $\alpha/\beta$  hydrolase fold. Microbial HSLs has been classified into two subfamilies, namely, GDSAG motif subfamily and GTSAG motif subfamily based on the conserved serine around the pentapeptide motif [24]. Most of the microbial HSL esterases so far reported belongs to GDSAG subfamily and are capable of forming dimers or oligomers in solution. Oligomerization involves hydrogen bonds and hydrophobic interactions involving antiparallel  $\beta$ 8 sheets and preceding  $\alpha$  helices of catalytic domain without the involvement of CAP domain [39, 42]. It was reported that in GDSAG subfamily dimerization may not be essential for catalysis, because both substrate binding pocket and active sites are away from the dimeric interface [24, 39, 43].

In the case of hyperthermophiles Pest E, Est 1, and AF-Est, the dimerization contributes to thermal stability [42]. In GTSAG subfamily, only one structure Est 25 (PDB ID:4Q05) has been reported. Dimerization pattern differs from the usual HSL oligomers that involve both the CAP and catalytic domain for dimerization. By site-directed mutagenesis at D224 in monomer B, it was confirmed that dimerization exerts its catalytic activity by correct positioning of the catalytic residue Asp 282 in the active site and also have partial effect on substrate binding [24]. In Ca-Est, the catalytic serine around the pentapeptide motif was not present either in GTSAG or GDSAG motif subfamilies of hormone-sensitive lipase [44, 45] that might belong to new member of microbial HSL.

A putative Ca\_C0816 gene from *Clostridium acetobutylicum* encoding for a protein with 242 amino acids was over-expressed in *E. Coli* strain BL21 and purified with affinity chromatography using  $\text{Ni}^{+2}$ -NTA resin after IPTG induction. Microbial HSL esterases exhibits oligomeric state in solution from monomer to tetramer [24], and Ca-Est was found to be a homodimer with a subunit size of 29 kDa which is within the range of molecular weights (20–69 kDa) of other microbial esterases reported in the literature [24, 46]. Ca-Est exhibited optimum pH 7.0 which is typically observed in microbial HSL esterases [44, 47] and optimum temperature at 60 °C. Based on the secondary structural spectra by CD spectroscopy, the enzyme was found stable at 60 °C (Fig. 5) with specific activity of 2403 U/mg with *p*-NPB. It is an unusual finding, where a mesophilic protein recorded an optimum activity at a moderately high temperature of 60 °C and thermal denaturation at 65 °C. However, there have been

cases of a mesophilic protein exhibiting high optimum temperature [48]. The melting temperature of wild-type Ca-Est was found to be 67.9 °C from CD spectroscopy. Thermal stability data showed that Ca-Est has half-life of 17.86 min at 60 °C. Ca-Est showed hydrolase activity towards small-to-medium acyl length of *p*-nitrophenyl esters from C2 to C8, but exhibited high activity for *p*-nitrophenyl butyrate, suggesting that this enzyme is an esterase rather than lipase [4, 45, 49, 50]. It also showed activity towards aryl esters such as  $\alpha$ -naphthyl acetate,  $\beta$ -naphthyl acetate, and 4-methylumbelliferyl acetate, but showed strict substrate preference towards  $\alpha$ -naphthyl acetate over  $\beta$ -naphthyl acetate. In addition, no detectable activity towards phenylacetate and little activity towards thioesterase. Mostly HSL esterases showed high activity towards *p*-nitrophenyl butyrate due to the funnel-shaped substrate binding pocket [51] which correlates with previously reported literature on esterase from other strains such as metagenomics library [45] *Rheinheimera* sp. [31] and Est25 from marine metagenomics [24]. In our study, this Ca-Est showed high  $k_{\text{cat}}$  for *p*-nitrophenyl butyrate when compared with other microbial esterases such as *Archaeoglobusfulgidus* [52], *Rhizomucor mehei* [27] and *Lactobacillus plantarum* [33]. Our data showed that Ca-Est was able to hydrolyse carboxylacidesters and arylesters.

The inhibitory effect of amino acid modifiers PMSF and DEPC confirmed that serine and histidine were very crucial for enzyme activity. The catalytic role of Ser89 and His224 was further confirmed by site-directed mutagenesis which confirmed that the serine conserved in a pentapeptide sequence GX SXG plays catalytic role in catalytic mechanism as reported for rat HSL [53] and His acts as a base in catalysis [35].

The secondary structure prediction of PDB3E0X (Fig. S2) shows an  $\alpha/\beta$  hydrolase fold. It has 13 helices with 7 strands and 1 sheet. The interconnectivity of the protein is maintained by 21 beta turns and 3 gamma turns and 18 helix–helix interactions. The uniqueness lies in the presence of a psi loop and a beta bulge of 6 amino acid length. The domain connectivity is depicted (Fig S1). The protein exists as a dimer, which was confirmed by gel filtration chromatography. The monomeric structure consists of two major domains, namely, catalytic and CAP domain. The catalytic domain consists of a typical alpha–beta hydrolase fold and is composed of seven  $\beta$  strands enclosed by nine  $\alpha$  helices ( $\alpha 1$ – $\alpha 4$ ) and ( $\alpha 9$ – $\alpha 13$ ). The CAP domain consists of alpha-helices ( $\alpha 5$ – $\alpha 8$ ) as described [54]. Analysis of amino acid composition shows that the protein is Leu-rich protein (12.2%) followed by Lys (10.6%), Ile (9.0%), Val (7.8%) and Glu (7.8%) using pdbparam online webserver. *p*-NPB with Ca-Est showed that the substrate-binding pocket is majorly surrounded by Leu and other hydrophobic residues that facilitate the binding of hydrophobic substrate molecules using AutoDock software 2.0 (Fig S3). We hypothesized

that the Ca-Est might have funnel shape substrate-binding pocket, so it allows the entry of < 10 carbon *p*-nitrophenyl esters.

Tolerance of Ca-Est with different detergents and organic solvents was investigated for its industrial applications. Ca-Est exhibited inactivation with organic solvents such as isopropanol, acetone, and ethanol, because these water-miscible organic solvents remove the water molecule around the enzyme, that eventually results in disruption of protein conformation and inactivate the enzyme activity. The Ca-Est activity was enhanced in the presence of 10% methanol; this might be due to the increase in the hydrogen bond interactions between enzyme surface and water molecules that could enhance the stability of enzymes in organic solvents [55]. Hence, it can be used in the transesterification reaction for the production of biodiesel or organic synthesis that have industrial applications [56–58]. For lipolytic enzymes, both detergents and their concentration helps either to enhance activity by promoting the emulsification and mixed micelles that aids in conformational changes of the enzyme, so that active site is accessible or to reduce the enzymatic activity due to the formation of inactive enzyme surfactant or by impairing the active binding site of enzyme at the interface [59]. Ionic detergent such as SDS had an inhibitory effect on Ca-Est activity, as it modifies the tertiary structure of the protein, whereas non-ionic detergents were less effective at disrupting the protein aggregation [60]. The enzyme showed more inactivation with Fe<sup>+2</sup> and Cu<sup>+2</sup> as compared to other metal ions. The complete loss of esterase activity might be due to Cys 24 adjacent to its catalytic triad as reported in the literature [61]. This effect has also been observed in other lipolytic enzymes [62]. It has been reported that some metal ions act as non-competitive inhibitors, destabilize the conformation of enzyme, and reduce the activity [63]. From the above findings, it can be concluded that this Ca-Est is a robust enzyme that withstands high temperatures and is active in the presence of methanol. These properties make it a valuable biocatalyst in the synthesis of biodiesel.

## Conclusions

There is a high demand for the screening of novel microbial lipolytic enzymes with superior properties. In this study, *Clostridium acetobutylicum* esterase (Ca-Est) contains a novel sequence GYSMG and HGSG motif that appears to be a new member of lipolytic family IV of hormone-sensitive lipase with catalytic serine found in GYSMG consensus motif. Ca-Est is a mesophilic enzyme, but showed high specific activity at a moderately high temperature of 60 °C. It also showed enhanced activity in the presence of methanol. Hence, this solvent tolerant esterase can prove to

be an attractive biocatalyst in the synthesis of biodiesel and biopolymers.

**Acknowledgements** Authors acknowledge IIT Madras for the facilities. Author N. Vijaya Lakshmi acknowledges AICTE-QIP and JNTUA College of Engineering Pulivendula.

**Funding** The researcher did not receive any specific grant from funding agencies in the public, commercial, or not for profit sectors.

## Compliance with ethical standards

**Conflict of interest** The authors declare that they have no conflict of interest.

**Ethical approval** This article does not contain any studies with human participants or animals performed by any one of the authors.

## References

1. Tao W, Shengxue F, Duobin M et al (2013) Characterization of a new thermophilic and acid tolerant esterase from *Thermotoga maritima* capable of hydrolytic resolution of racemic ketoprofen ethyl ester. *J Mol Catal B Enzym* 85–86:23–30. <https://doi.org/10.1016/j.molcatb.2012.08.006>
2. Javed S, Azeem F, Hussain S et al (2018) Bacterial lipases: a review on purification and characterization. *Prog Biophys Mol Biol* 132:23–34. <https://doi.org/10.1016/j.pbiomolbio.2017.07.014>
3. Chen C-C, Chi Z, Liu G-L et al (2017) Production, purification, characterization and gene cloning of an esterase produced by *Aureobasidium melanogenum* HN6.2. *Process Biochem* 53:69–79. <https://doi.org/10.1016/j.procbio.2016.12.006>
4. Arpigny JL, Jaeger KE (1999) Bacterial lipolytic enzymes: classification and properties. *Biochem J* 343(Pt 1):177–183
5. Casas-Godoy L, Duquesne S, Bordes F et al (2012) Lipases: an overview. In: Sandoval G (ed) *Lipases and phospholipases*. Humana Press, Totowa, pp 3–30
6. Jayanath G, Mohandas SP, Kachiprath B et al (2018) A novel solvent tolerant esterase of GDSGG motif subfamily from solar saltern through metagenomic approach: recombinant expression and characterization. *Int J Biol Macromol* 119:393–401. <https://doi.org/10.1016/j.ijbiomac.2018.06.057>
7. Ramnath L, Sithole B, Govinden R (2017) Classification of lipolytic enzymes and their biotechnological applications in the pulping industry. *Can J Microbiol* 63:179–192. <https://doi.org/10.1139/cjm-2016-0447>
8. Singh R, Kumar M, Mittal A, Mehta PK (2016) Microbial enzymes: industrial progress in 21st century. *3 Biotech*. <https://doi.org/10.1007/s13205-016-0485-8>
9. Sarmah N, Revathi D, Sheelu G et al (2018) Recent advances on sources and industrial applications of lipases: biotechnol. *Prog.*, 2017, Vol. 00, No. 00. *Biotechnol Prog* 34:5–28. <https://doi.org/10.1002/btpr.2581>
10. Ferrer M, Bargiela R, Martínez-Martínez M et al (2015) Biodiversity for biocatalysis: a review of the  $\alpha/\beta$ -hydrolase fold superfamily of esterases-lipases discovered in metagenomes. *Biocatal Biotransform* 33:235–249. <https://doi.org/10.3109/10242422.2016.1151416>
11. Navvabi A, Razzaghi M, Fernandes P et al (2018) Novel lipases discovery specifically from marine organisms for industrial

- production and practical applications. *Process Biochem* 70:61–70. <https://doi.org/10.1016/j.procbio.2018.04.018>
12. Kovacic F, Babic N, Krauss U, Jaeger K-E (2019) Classification of lipolytic enzymes from bacteria. In: Rojo F (ed) *Aerobic utilization of hydrocarbons, oils and lipids*. Springer International Publishing, Cham, pp 1–35
  13. Lenfant N, Hotelier T, Velluet E et al (2013) ESTHER, the database of the  $\alpha/\beta$ -hydrolase fold superfamily of proteins: tools to explore diversity of functions. *Nucleic Acids Res* 41:D423–D429. <https://doi.org/10.1093/nar/gks1154>
  14. Hotelier T (2004) ESTHER, the database of the  $\alpha$ -hydrolase fold superfamily of proteins. *Nucleic Acids Res* 32:145D–147D. <https://doi.org/10.1093/nar/gkh141>
  15. Lampidonis AD, Rogdakis E, Voutsinas GE, Stravopodis DJ (2011) The resurgence of Hormone-Sensitive Lipase (HSL) in mammalian lipolysis. *Gene* 477:1–11. <https://doi.org/10.1016/j.gene.2011.01.007>
  16. Lass A, Zimmermann R, Oberer M, Zechner R (2011) Lipolysis—a highly regulated multi-enzyme complex mediates the catabolism of cellular fat stores. *Prog Lipid Res* 50:14–27. <https://doi.org/10.1016/j.plipres.2010.10.004>
  17. Langin D, Laurell H, Holst LS et al (1993) Gene organization and primary structure of human hormone-sensitive lipase: possible significance of a sequence homology with a lipase of *Moraxella TA144*, an antarctic bacterium. *Proc Natl Acad Sci USA* 90:4897–4901
  18. Kim TD (2017) Bacterial hormone-sensitive lipases (bHSLs): emerging enzymes for biotechnological applications. *J Microbiol Biotechnol* 27:1907–1915. <https://doi.org/10.4014/jmb.1708.08004>
  19. Osterlund T (2001) Structure-function relationships of hormone-sensitive lipase. *Eur J Biochem* 268:1899–1907
  20. Østerlund T, Contreras JA, Holm C (1997) Identification of essential aspartic acid and histidine residues of hormone-sensitive lipase: apparent residues of the catalytic triad. *FEBS Lett* 403:259–262. [https://doi.org/10.1016/S0014-5793\(97\)00063-X](https://doi.org/10.1016/S0014-5793(97)00063-X)
  21. De Simone G, Galdiero S, Manco G et al (2000) A snapshot of a transition state analogue of a novel thermophilic esterase belonging to the subfamily of mammalian hormone-sensitive lipase 1 | Edited by D. Rees. *J Mol Biol* 303:761–771. <https://doi.org/10.1006/jmbi.2000.4195>
  22. Hemilä H, Koivula TT, Palva I (1994) Hormone-sensitive lipase is closely related to several bacterial proteins, and distantly related to acetylcholinesterase and lipoprotein lipase: identification of a superfamily of esterases and lipases. *Biochimica et Biophysica Acta (BBA) Lipids and Lipid Metabolism* 1210:249–253. [https://doi.org/10.1016/0005-2760\(94\)90129-5](https://doi.org/10.1016/0005-2760(94)90129-5)
  23. Noby N, Saeed H, Embaby AM et al (2018) Cloning, expression and characterization of cold active esterase (EstN7) from *Bacillus cohnii* strain N1: a novel member of family IV. *Int J Biol Macromol* 120:1247–1255. <https://doi.org/10.1016/j.ijbio mac.2018.07.169>
  24. Li P-Y, Ji P, Li C-Y et al (2014) Structural basis for dimerization and catalysis of a novel esterase from the GTSAG motif subfamily of the bacterial hormone-sensitive lipase family. *J Biol Chem* 289:19031–19041. <https://doi.org/10.1074/jbc.M114.574913>
  25. Jeon JH, Lee HS, Kim JT et al (2012) Identification of a new subfamily of salt-tolerant esterases from a metagenomic library of tidal flat sediment. *Appl Microbiol Biotechnol* 93:623–631. <https://doi.org/10.1007/s00253-011-3433-x>
  26. Kim B, Yoo W, Le Huong Luu LT et al (2019) Characterization and mutation analysis of a cold-active bacterial hormone-sensitive lipase from *Salinisphaera* sp. P7-4. *Arch Biochem Biophys* 663:132–142. <https://doi.org/10.1016/j.abb.2019.01.010>
  27. Liu Y, Xu H, Yan Q et al (2013) Biochemical characterization of a first fungal esterase from *rhizomucor miehei* showing high efficiency of ester synthesis. *PLoS One* 8:e77856. <https://doi.org/10.1371/journal.pone.0077856>
  28. Manco G, Giosuè E, D'Auria S et al (2000) Cloning, overexpression, and properties of a new thermophilic and thermostable esterase with sequence similarity to hormone-Sensitive Lipase subfamily from the Archaeon *Archaeoglobus fulgidus*. *Arch Biochem Biophys* 373:182–192. <https://doi.org/10.1006/abbi.1999.1497>
  29. Li C, Li Q, Zhang Y et al (2017) Characterization and function of *Mycobacterium tuberculosis* H37Rv Lipase Rv1076 (LipU). *Microbiol Res* 196:7–16. <https://doi.org/10.1016/j.micres.2016.12.005>
  30. Zarafeta D, Moschidi D, Ladoukakis E et al (2016) Metagenomic mining for thermostable esterolytic enzymes uncovers a new family of bacterial esterases. *Sci Rep*. <https://doi.org/10.1038/srep38886>
  31. Virk AP (2011) A new esterase, belonging to hormone-sensitive lipase family, cloned from *Rheinheimera* sp. isolated from industrial effluent. *J Microbiol Biotechnol* 21:667–674. <https://doi.org/10.4014/jmb.1103.03008>
  32. Sánchez-Carbente MDR, Batista-García RA, Sánchez-Reyes A et al (2017) The first description of a hormone-sensitive lipase from a basidiomycete: structural insights and biochemical characterization revealed *Bjerkandera adusta* Ba EstB as a novel esterase. *MicrobiologyOpen* 6:e00463. <https://doi.org/10.1002/mbo3.463>
  33. Alvarez Y, Esteban-Torres M, Cortés-Cabrera Á et al (2014) Esterase LpEst1 from *Lactobacillus plantarum*: a novel and atypical member of the  $\alpha\beta$  hydrolase superfamily of enzymes. *PLoS One* 9:e92257. <https://doi.org/10.1371/journal.pone.0092257>
  34. Emtenani S, Asoodeh A, Emtenani S (2013) Molecular cloning of a thermo-alkaliphilic lipase from *Bacillus subtilis* DR8806: expression and biochemical characterization. *Process Biochem* 48:1679–1685. <https://doi.org/10.1016/j.procbio.2013.08.016>
  35. Choi Y-H, Lee Y-N, Park Y-J et al (2016) Identification of amino acids related to catalytic function of *Sulfolobus solfataricus* P1 carboxylesterase by site-directed mutagenesis and molecular modeling. *BMB Rep* 49:349–354. <https://doi.org/10.5483/BMBRep.2016.49.6.077>
  36. Lee J, Jang Y-S, Choi SJ et al (2012) Metabolic engineering of *Clostridium acetobutylicum* ATCC 824 for isopropanol-butanol-ethanol fermentation. *Appl Environ Microbiol* 78:1416–1423. <https://doi.org/10.1128/AEM.06382-11>
  37. Schwarz KM, Kuit W, Grimmmer C et al (2012) A transcriptional study of acidogenic chemostat cells of *Clostridium acetobutylicum*—cellular behavior in adaptation to n-butanol. *J Biotechnol* 161:366–377. <https://doi.org/10.1016/j.jbiotec.2012.03.018>
  38. Rehdorf J, Behrens GA, Nguyen G-S et al (2012) *Pseudomonas putida* esterase contains a GGG(A)X-motif conferring activity for the kinetic resolution of tertiary alcohols. *Appl Microbiol Biotechnol* 93:1119–1126. <https://doi.org/10.1007/s00253-011-3464-3>
  39. Palm GJ, Fernández-Álvarez E, Bogdanović X et al (2011) The crystal structure of an esterase from the hyperthermophilic microorganism *Pyrobaculum caldifontis* VA1 explains its enantioselectivity. *Appl Microbiol Biotechnol* 91:1061–1072. <https://doi.org/10.1007/s00253-011-3337-9>
  40. Mandrich L, Merone L, Pezzullo M et al (2005) Role of the N terminus in enzyme activity, stability and specificity in thermophilic esterases belonging to the HSL family. *J Mol Biol* 345:501–512. <https://doi.org/10.1016/j.jmb.2004.10.035>
  41. Bassegoda A, Fillat A, Pastor FJ, Diaz P (2013) Special *Rhodococcus* sp. CR-53 esterase Est4 contains a GGG(A)X-oxyanion hole conferring activity for the kinetic resolution of tertiary alcohols. *Appl Microbiol Biotechnol* 97:8559–8568. <https://doi.org/10.1007/s00253-012-4676-x>
  42. Byun J-S, Rhee J-K, Kim N et al (2007) Crystal structure of hyperthermophilic esterase EstE1 and the relationship between

- its dimerization and thermostability properties. *BMC Struct Biol* 7:47. <https://doi.org/10.1186/1472-6807-7-47>
43. De Simone G, Menchise V, Manco G et al (2001) The crystal structure of a hyper-thermophilic carboxylesterase from the archaeon *Archaeoglobus fulgidus* 1 | Edited by R. Huber. *J Mol Biol* 314:507–518. <https://doi.org/10.1006/jmbi.2001.5152>
  44. Huo Y-Y, Jian S-L, Cheng H et al (2018) Two novel deep-sea sediment metagenome-derived esterases: residue 199 is the determinant of substrate specificity and preference. *Microb Cell Fact*. <https://doi.org/10.1186/s12934-018-0864-4>
  45. Petrovskaya LE, Novototskaya-Vlasova KA, Spirina EV et al (2016) Expression and characterization of a new esterase with GCSAG motif from a permafrost metagenomic library. *FEMS Microbiol Ecol* 92:fiw046. <https://doi.org/10.1093/femsec/fiw046>
  46. Benavente R, Esteban-Torres M, Acebrón I et al (2013) Structure, biochemical characterization and analysis of the pleomorphism of carboxylesterase Cest-2923 from *Lactobacillus plantarum* WCFS1. *FEBS J* 280:6658–6671. <https://doi.org/10.1111/febs.12569>
  47. Neves Petersen MT, Fojan P, Petersen SB (2001) How do lipases and esterases work: the electrostatic contribution. *J Biotechnol* 85:115–147. [https://doi.org/10.1016/S0168-1656\(00\)00360-6](https://doi.org/10.1016/S0168-1656(00)00360-6)
  48. Declerck N, Machius M, Wiegand G et al (2000) Probing structural determinants specifying high thermostability in *Bacillus licheniformis* alpha-amylase. *J Mol Biol* 301:1041–1057. <https://doi.org/10.1006/jmbi.2000.4025>
  49. Bornscheuer UT (2002) Microbial carboxyl esterases: classification, properties and application in biocatalysis. *FEMS Microbiol Rev* 26:73–81. <https://doi.org/10.1111/j.1574-6976.2002.tb00599.x>
  50. Ghata A, Paul G (2015) Purification and characterization of a thermo-halophilic, alkali-stable and extremely benzene tolerant esterase from a thermo-halo tolerant *Bacillus cereus* strain AGP-03, isolated from ‘Bakreshwar’ hot spring, India. *Process Biochem* 50:771–781. <https://doi.org/10.1016/j.procbio.2015.01.026>
  51. Yang S, Qin Z, Duan X et al (2015) Structural insights into the substrate specificity of two esterases from the thermophilic *Rhizomucor miehei*. *J Lipid Res* 56:1616–1624. <https://doi.org/10.1194/jlr.M060673>
  52. Sayer C, Finnigan W, Isupov MN et al (2016) Structural and biochemical characterisation of *Archaeoglobus fulgidus* esterase reveals a bound CoA molecule in the vicinity of the active site. *Sci Rep*. <https://doi.org/10.1038/srep25542>
  53. Holm C, Davis RC, Osterlund T et al (1994) Identification of the active site serine of hormone-sensitive lipase by site-directed mutagenesis. *FEBS Lett* 344:234–238
  54. Lee CW, Kwon S, Park S-H et al (2017) Crystal structure and functional characterization of an esterase (EaEST) from *Exiguobacterium antarcticum*. *PLoS One* 12:e0169540. <https://doi.org/10.1371/journal.pone.0169540>
  55. Park HJ, Joo JC, Park K, Yoo YJ (2012) Stabilization of *Candida antarctica* lipase B in hydrophilic organic solvent by rational design of hydrogen bond. *Biotechnol Bioprocess Eng* 17:722–728. <https://doi.org/10.1007/s12257-012-0092-4>
  56. Alex D, Shainu A, Pandey A, Sukumaran RK (2014) Esterase Active in Polar Organic Solvents from the Yeast *Pseudozyma* sp. NII 08165. *Enzyme Res* 2014:1–10. <https://doi.org/10.1155/2014/494682>
  57. Fan X, Niehus X, Sandoval G (2012) Lipases as biocatalyst for biodiesel production. In: Sandoval G (ed) *Lipases and phospholipases*. Humana Press, Totowa, pp 471–483
  58. Sivaramakrishnan R, Muthukumar K (2012) Isolation of thermostable and solvent-tolerant bacillus sp. lipase for the production of biodiesel. *Appl Biochem Biotechnol* 166:1095–1111. <https://doi.org/10.1007/s12010-011-9497-3>
  59. Delorme V, Dhoub R, Canaan S et al (2011) Effects of surfactants on lipase structure, activity, and inhibition. *Pharm Res* 28:1831–1842. <https://doi.org/10.1007/s11095-010-0362-9>
  60. Neugebauer JM (1990) Detergents: an overview. *Meth Enzymol* 182:239–253
  61. Legler PM, Leary DH, Hervey WJ, Millard CB (2012) A role for His-160 in peroxide inhibition of *S. cerevisiae* S-formylglutathione hydrolase: evidence for an oxidation sensitive motif. *Arch Biochem Biophys* 528:7–20. <https://doi.org/10.1016/j.abb.2012.08.001>
  62. Jeon JH, Kim J-T, Kang SG et al (2009) Characterization and its potential application of two esterases derived from the arctic sediment metagenome. *Mar Biotechnol* 11:307–316. <https://doi.org/10.1007/s10126-008-9145-2>
  63. Asoodeh A, Ghorani Azam A, Zardini H (2014) Biochemical characterization of a novel thermophilic esterase isolated from *Shewanella* sp F88. *J Sci Repub Iran* 25(1):5–12

**Publisher's Note** Springer Nature remains neutral with regard to jurisdictional claims in published maps and institutional affiliations.